

Article

Influence of the Addition of Sialon and Aluminum Nitride Fillers on the Photocuring Process of Polymer Coatings

Mariola Robakowska ^{1,*}, Łukasz Gierz ^{2,*}, Paulina Mayer ³, Katarzyna Szcześniak ^{1,4},
Agnieszka Marcinkowska ¹, Aneta Lewandowska ¹ and Piotr Gajewski ¹

¹ Faculty of Chemical Technology, Poznań University of Technology, 60-965 Poznań, Poland

² Institute of Machine Design, Faculty of Mechanical Engineering, Poznań University of Technology, Piotrowo 3, 60-965 Poznań, Poland

³ Faculty of Mechanical Engineering, Wrocław University of Science and Technology, Wybrzeże Wyspiańskiego 27, 50-370 Wrocław, Poland

⁴ NanoBioMedical Center, Adam Mickiewicz University, Wszechnicy Piastowskiej 3, 61-614 Poznań, Poland

* Correspondence: mariola.robakowska@put.poznan.pl (M.R.); lukasz.gierz@put.poznan.pl (Ł.G.);
Tel.: +48-61-6653683 (M.R.); +48-61-2244516 (Ł.G.); Fax: +48-61-6653649 (M.R.)

Abstract: This article presents the results of a study on polymer coatings containing poly ethoxylated bisphenol A diacrylate (Bis-AEA10) with aluminum silicon nitride oxide (Sialon) and aluminum nitride (AlN). The polymer coatings were obtained by the photopolymerization technique. Investigations were carried out to determine the effect of the AlN and Sialon content on the UV-curing kinetics, as well as on the mechanical (hardness), thermal (T_g , thermal stability), physicochemical (water contact angle), and structural properties of the polymer coatings. Polymerization rates were characterized as functions of double-bond conversion using the photo-Differential Scanning Calorimetry technique (photo-DSC). The results obtained showed that a small addition of sialon filler (3–5 wt.%) to Bis-AEA10 increases the photopolymerization rate of the varnish, while the addition of more Sialon decreases the rate of photopolymerization. However, for the systems containing AlN filler, the maximum polymerization rate was observed for samples containing 10 wt.% filler. In the case of a varnish composition containing AlN, the maximum polymerization rate is characterized by the system containing 10 wt.% of AlN. This shows that the AlN filler has a good influence on the polymerization process. In either case, the final double bond conversion was high (80%–95%). Mechanical tests have shown that introducing the filler into the polymer matrix increases its hardness. The content of Sialon and AlN in the coatings causes an increase (up to 4–5 wt.%) and a decrease (>4–5 wt.%) in the glass transition temperature. The effect of the addition of fillers on the physicochemical properties of the coating surface has also been investigated and characterized by the water contact angle method. The addition of 20 wt.% Sialon and AlN increased the contact angle of the samples by approximately 40% and 31%, respectively, resulting in coatings with hydrophobic surface properties.

Keywords: aluminum nitride; sialon; UV-curable coating; UV-curing kinetics; hydrophobicity; thermal properties; surface wettability



Citation: Robakowska, M.; Gierz, Ł.; Mayer, P.; Szcześniak, K.; Marcinkowska, A.; Lewandowska, A.; Gajewski, P. Influence of the Addition of Sialon and Aluminum Nitride Fillers on the Photocuring Process of Polymer Coatings. *Coatings* **2022**, *12*, 1389. <https://doi.org/10.3390/coatings12101389>

Academic Editor: Günter Motz

Received: 22 July 2022

Accepted: 20 September 2022

Published: 22 September 2022

Publisher's Note: MDPI stays neutral with regard to jurisdictional claims in published maps and institutional affiliations.



Copyright: © 2022 by the authors. Licensee MDPI, Basel, Switzerland. This article is an open access article distributed under the terms and conditions of the Creative Commons Attribution (CC BY) license (<https://creativecommons.org/licenses/by/4.0/>).

1. Introduction

Aluminum silicon nitride oxide (Sialon) has a complex chemistry and should be considered as a family of alloys with a broad range of properties, e.g., good high-temperature strength, high fracture toughness, strength, and corrosion resistance, which have been widely used as engineering ceramics, cutting tools, and refractory materials. Sialons are formed when silicon nitride, aluminum nitride, and aluminum oxide are prepared by the hot-press sintering method.

Sialon is an excellent oxy-nitride ceramic due to its unique combination of high Young's modulus (270–275 GPa), moderate hardness (15–17 GPa) and high fracture toughness

(6–8 MPa) [1]. Most related work focuses on the synthesis and optimization of experimental conditions for the synthesis of various Sialon materials [1–4]. Researchers have used many additives to achieve desirable physical, thermal, mechanical and wear-resistant characteristics of Sialon-based materials [2,5–7]. The above-mentioned ceramic materials are commonly used for cutting tools, mechanical seals, heat exchangers, and ingredients for heat engines, generally in the form of monolithic material [8]. Among the various fillers, which are part of the Sialon particles, aluminum nitride (AlN) is an important ceramic material that is in great demand due to its excellent thermal conductivity (82–170 W/mK), electrical resistance ($>10^{14} \Omega \cdot \text{cm}$), as well as its thermal stability, lack of toxicity, silicon-like low coefficient of thermal expansion, good chemical stability and high hardness [9–12].

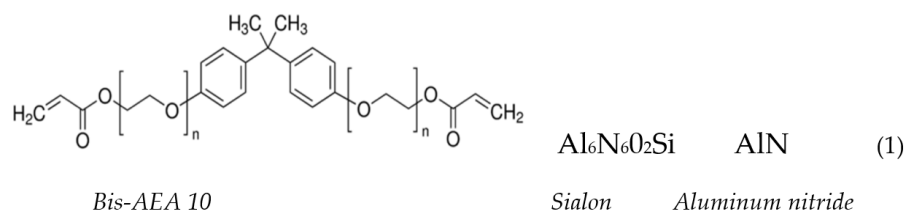
An easier way to disperse fillers in a polymer matrix is to prepare the composite in situ, by the polymerization of the monomer (or mixture of monomers) containing dispersed additive [13–15]. The particularly interesting method is photopolymerization because of its high-speed reaction rate, low temperature of the process, and solvent-free composition. The polymerization process takes place only in the area exposed to direct light, which allows the process to be controlled and does not require the use of additional solvents. These advantages of photopolymerization in combination with the incorporation of inorganic particles into the photocurable system are an attractive method for the generation of high-performance coatings [13–17]. UV polymerization has been used in applications, especially in surface coatings and adhesives. Although some studies have investigated the formation of UV-induced inorganic coatings, the effect of the filler on the polymerization rate of these systems was often overlooked. In our previous work [12], we used sialon (and aluminum oxide) as fillers for polymer coatings. We noticed that the addition of small amounts (5 wt.%) of inorganic compounds improved the hydrophobicity of the polymer coating surface, scratch resistance, scratch hardness, and surface hydrophobicity. In these coatings, SEM and AFM imaging showed a very fine distribution of fillers in the matrix studied.

This study was concentrated on the synthesis and characterization of coatings containing Sialon and AlN. Hybrid organic-inorganic coatings have been obtained by polymerization of ultraviolet (UV) curable systems containing different contents of Sialon, AlN, and bisphenol A diacrylate (Bis-AEA10). Photocuring kinetic analysis of UV-initiated photopolymerizations of the acrylate system with and without fillers using photo-differential scanning calorimetry (photo-DSC) was examined. Kinetic studies were complemented by measurements of the formed thermal properties of the coatings and their selected mechanical properties. This paper also presents the results of using a scanning electron microscope (SEM) to study changes in the bulk morphology of the coatings. To the best of our knowledge, there are no specific data on the photocuring behavior of systems containing Sialon and aluminum nitride. It is known that the incorporation of aluminum nitride (aluminum solid nitride) into the composite significantly contributes to increasing stiffness, thermal conductivity and reducing thermal expansion of the composites [18]. The chemical properties of Sialon correspond to those of aluminum nitride (for example, it has a high resistance to oxidation at elevated temperatures), so in this article we will compare the influence of both fillers on physicochemical and thermal parameters. Our investigations can help design polymer coatings containing Sialon and AlN for use in industrial sectors.

2. Materials and Methods

2.1. Materials

The monomer: ethoxylated bisphenol A diacrylate (Bis-AEA10, purity 96%, Scheme 1) and the photoinitiator: 2,2-dimethoxy-2-phenylacetophenone (Irgacure 651) were kindly donated by Sigma-Aldrich (Saint Louis, MO, USA). Bis-AEA10 is a highly reactive difunctional diacrylate ester, which is polymerized by a common free radical initiator. The product can be easily applied to wood and metal material and can provide chemical resistance and corrosion resistance, increased external durability, and flexibility.



Scheme 1. Reagent formulas.

Aluminum nitride (in the form of nanopowder with a particle size < 100 nm) and Sialon ($\text{Al}_6\text{N}_6\text{O}_2\text{Si}$, microsized) were purchased from Sigma Aldrich. The fillers were dried at 110 °C for 2 h prior to use. Monomer/filler system containing 0–20 wt.% Sialon/AlN and 0.2 wt.% of the photoinitiator were homogenized by ultrasonication for 3–22 h.

2.2. Viscosity

The viscosity of the composition was measured with a Brookfield RVDV-II + Pro cone/plate viscometer with thermostat. Viscosity was measured at temperatures of 20, 25, 30, 40 and 50 °C and various rotational speeds of the cone (10–200 rpm).

2.3. Photopolymerization Kinetics

The curing kinetics were measured by DSC under isothermal conditions at 25 ± 0.01 °C in a high purity argon atmosphere (<0.0005% of O_2) using the Pyris 6 instrument (Perkin-Elmer, Waltham, MA, USA) equipped with a specially designed lid for photochemical measurements. The 2 mg samples were polymerized in open aluminum pans with diameter of 6.6 mm. Polymerizations were initiated by the light from the Hamamatsu LC-L1 lamp (365 nm, the light intensity in the sample pan was 2.75 mWcm^{-2}). The photoinitiator concentration was 0.2 wt.%. All photopolymerization experiments were conducted at least in triplicate. For computations, the polymerization heat was taken to be 86 kJmol^{-1} per double bond [19].

2.4. Thermal Properties

The glass transition temperature T_g was measured with a DSC instrument (DSC1 Mettler Toledo, Columbus, OH, USA) under a nitrogen atmosphere at a heating rate of 20 °C/min. The 5 mg samples were scanned at a heating rate of 20 °C min^{-1} in a temperature range from –40 to 110 °C (the sample was kept for 5 min at 110 °C and –40 °C). T_g was evaluated from the second run of two separate DSC measurements.

Thermal resistance was investigated with a TG 209 F3 Tarsus thermogravimetric analyzer (NETZSCH-Geratebau GmbH, Selb, Germany). The 10 mg samples were heated in Al_2O_3 crucibles from 40 to 600 °C at a scan rate of 10 °C/min in a nitrogen atmosphere (purge of 10 mL/min of N_2 protection gas and 20 mL/min of N_2 sample gas).

2.5. Mechanical Properties

The samples for mechanical tests were cured in a two-part stainless-steel mold. The samples in the mold were covered with poly(ethylene terephthalate) foil. The BisEA10/filler compositions were irradiated with the entire spectrum of the Dymax UV 5000 Flood lamp for 300 s. Shore D hardness was measured according to DIN 53 505.

2.6. FTIR Analysis

Fourier-transform infrared (FTIR) spectra of the products were obtained using the attenuated total reflectance (ATR) mode (a Nicolet 5700 equipped with a ZnSe crystal ATR unit, Thermo Fisher Scientific Inc., Waltham, MA, USA and a Bruker Tensor 27 equipped with a SPECAC Golden Gate diamond ATR accessory, Bruker Optiks GmbH, Ettlingen, Germany). Spectra were recorded with a resolution of 4 cm^{-1} and an accumulation of 64 spectra.

2.7. SEM

The morphology of all fillers and composite was investigated using a JEOL 7001F scanning electron microscope (Akishima, Tokyo, Japan, SEI detector, 7 kV accelerating voltage). Before measurement, small pieces of each sample were taken and placed on a stub of metal with carbon adhesive tape and then covered with an ultrathin gold coating applied to the samples by low-vacuum sputtering.

2.8. Surface Wettability

The water contact angle in the coatings was investigated using a sessile drop method using the OCA 15EC contact angle goniometer (DataPhysics Instruments GmbH, Filderstadt, Germany) at room temperature (approximately 25 °C) and with an accuracy ± 0.01 mN/m. Water droplets of 0.2 μ L were deposited at ten random locations in the coatings for each measurement. The droplet images were recorded and analyzed using the SCA shape analysis software (SCA20, SCA21, DataPhysics Instruments GmbH, Filderstadt, Germany).

3. Test Results and Discussion

The SEM images are shown in Figure 1. Both AlN and Sialon samples have irregular particles shapes. The particle size of AlN, as reported by the manufacturer, was <100 nm, while the sizes were generally characterized as micrometric. However, the particle sizes of both samples, measured by SEM, were much higher than those in the data sheets. Fundamental work on surface characterization of AlN nanopowders enabled an understanding of the surface chemical structures and reactivity of AlN nanoparticles; as revealed, there are hydroxyl and amine groups, as well as Lewis acid and base sites on the surface [20]. These surface chemical features cause an inevitable agglomerated structure, as shown in the SEM image (Figure 1). The SEM picture of the micro powder also shows also agglomerates of Sialon particles. Both fillers have some carrot-like particles, with lengths up to a few micrometers; however, in the case of aluminum nitride, nanometre-sized primary particles are also present. The size distribution of AlN varies from 200 nm up of ~ 10 μ m, however, most of the sizes in the distribution are located approximately between 1.0 and 2 μ m.

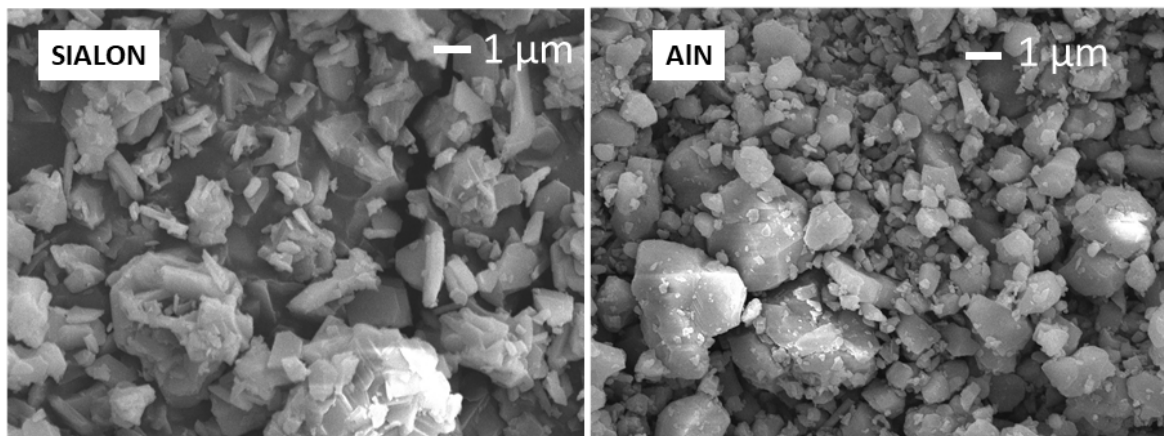


Figure 1. SEM images of the particles Sialon and AlN.

3.1. Viscosity Test

The viscosity of a UV-curable compositions is one of the most important parameters in the production of coatings because it affects both the curing chemistry and polymerization rate and is a fundamental factor in the correct application of the lacquer on the material surface. Ethoxylated bisphenol A diacrylate is a difunctional acrylate monomer designed for a wide variety of applications. BisEA10, which shows low odor and low volatility monomer and is used in free radical polymerization. The viscosity of the composition is crucial in the course of polymerization. Therefore, when preparing the composition of new filler varnishes, it is necessary to pay particular attention to the type of filler and the

amount of filler added, to obtain the desired viscosity of the composition [12]. Sialon is a silicon nitride ceramic with a small percentage of aluminum nitride added; therefore, we can say that Sialon are ceramic alloys containing the elements silicon (Si), aluminum (Al), oxygen (O), and nitrogen (N).

The viscosities of the compositions are shown in Figure 2: (a) the BisEA10/Sialon composition; (b) BisEA10/AlN composition (at 25 °C) and (c) the dependence of the viscosity on the filler content at the rotation speed $V = 60$ rpm. In our previous publication [12], the 1.5 wt.% of the Sialon filler added to the varnishes slightly reduced the viscosity of the composition, the larger amounts of Sialon (3 wt.% and 5 wt.%) increased the viscosity of the composition by 11% and 20% (at 25 °C), respectively, compared to the viscosity of the compositions without the filler. However, it was a mixture of other monomers with a viscosity lower than that in this publication. In the case of bisEA10 resin, the addition of 5 wt.% Sialon caused the viscosity of the composition to increase by 91% (at 25 °C shear rate ~ 60 rpm) and when the same amount of AlN was added, the viscosity of the composition increased by 38%. As can be seen, the composition viscosity increased with the filler concentration, more than a threefold increase when compared to the monomer, indicating a composition containing 20 wt.% of Sialon. Our coatings show some degree of pseudoplastic (shear-thinning) flow behavior. The non-Newtonian behavior of the formulation may be caused by several factors, all of which are related to the structural reorganization of the molecules of system due to the flow and formation of aggregates and clusters of particles that increase the effective volume fraction of the filler in the system. Segregation of different fillers and their quantity and size in the flow cause a shear thinning behavior below the shear rate ~ 50 rpm. The increase in viscosity stems mostly due to the interfacial friction between the fillers and between fillers and the dispersing medium. Due to Brownian movement or interactions that induce relative motion of particles, the microstructure can be rebuilt as the flow decreases or stops and, in some cases, forms a space-filling structure network [21].

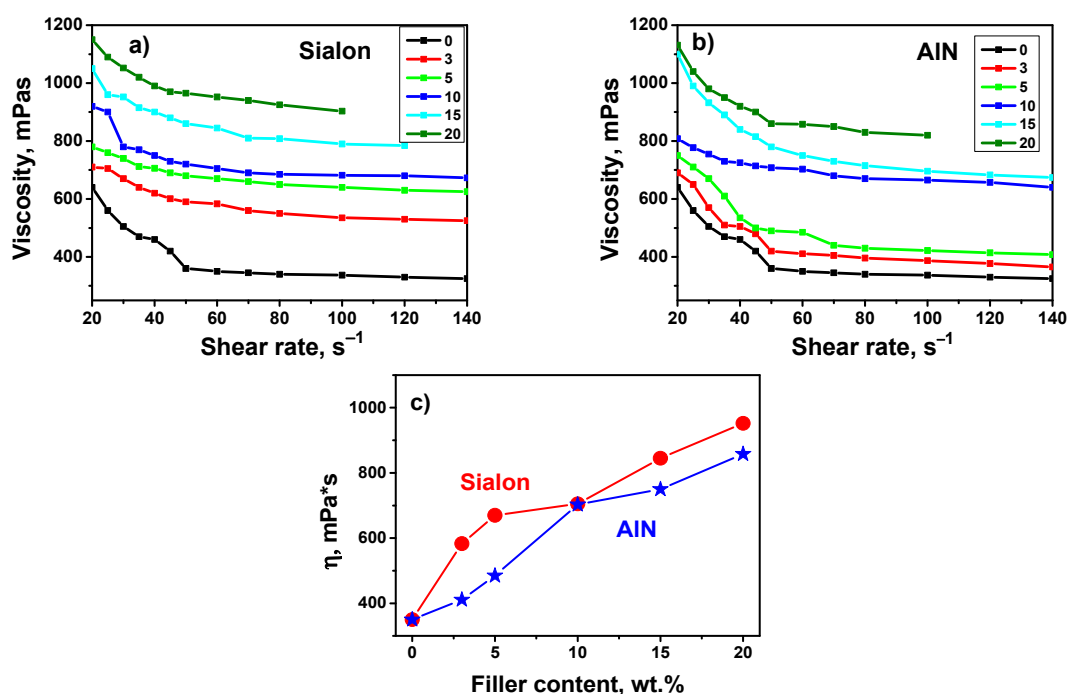


Figure 2. The viscosity of a composition as the function of the shear rate and the filler content at 25 °C; (a) Sialon, (b) AlN and the dependency of the viscosity of the formulation as the fillers content function at a shear rate ~ 60 rpm, (c) The numbers indicate the filler content as a weight percent. The lines are guides for the eye.

3.2. Photopolymerization Kinetics

The conversion-rate curves for the photopolymerization of formulations containing various amounts of Sialon and AlN are shown in Figure 3. Figure 3 shows the kinetic curves of photopolymerization in the system $R_p = f(p)$ (where p —is the degree of reaction, R_p —is the rate of polymerization). The shape of the curves corresponds to the kinetic curve of the polymerization of multifunctional monomers with immediate autoacceleration, the occurrence of a maximum reaction rate (R_p^{max}), and subsequent deceleration. R_p^{max} appears at ~20%–30% of double bond conversion. At this stage of the reaction, the termination mechanism changes: from translational diffusion to diffusion of the reaction as the dominant route [16]. The addition of each of the fillers influences the polymerization kinetics, but increasing the filler content does not cause a monotonic trend in changes in R_p^{max} . This parameter first increases and reaches the highest value (Figure 2c) for system containing 10 wt.% AlN; a further increase in the filler content slightly reduces the polymerization rate. The analysis of the curves in Figure 3 indicates that the addition of AlN causes an increase in the final bond conversion (p^f) (Figure 3d). These results show that aluminum nitride has a beneficial effect on the photopolymerization of the monomer used and may suggest that the system mobility (which determines the p^f value) also increases. This may be related, among others, to the increase in viscosity of the composition after the introduction of the filler (Figure 1). The termination rate coefficient is inversely proportional to the viscosity of the polymerization mixture; therefore, the higher the viscosity, the higher the reaction rate [13–15]. However, inhibition of polymerization with an aluminum nitride concentration may be caused by light scattering by the filler.

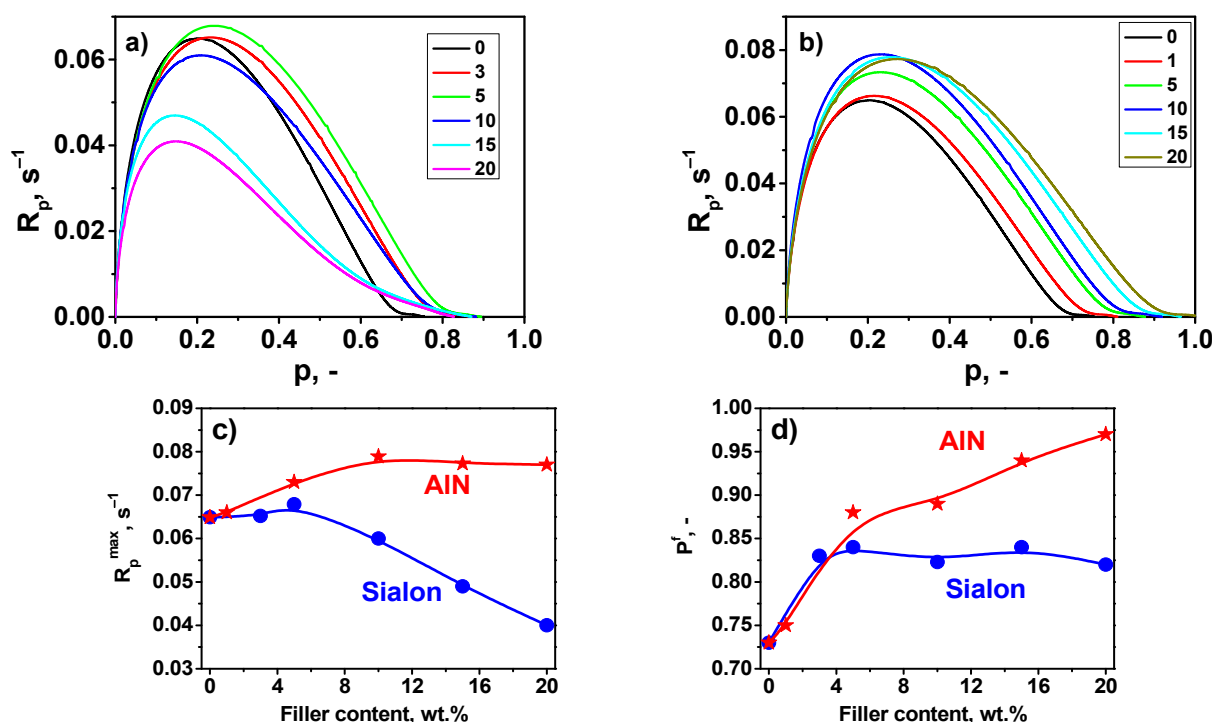


Figure 3. Dependence of the polymerization rate R_p on double bond conversion p (at 25 °C) for the: (a) monomer/Sialon, (b) monomer/AlN, (c) maximum polymerization rate R_p^{maks} , and (d) final bond conversion (p^f) for formulations at various filler content (in wt.%). The lines are guides for the eye.

Varnish compositions containing Sialon show a slightly different polymerization process. The positive effect of Sialon is very slight, and the slowing-down effect dominates. This is more apparent in Figure 2c showing the changes R_p^{max} of both compositions with an increasing content of filler. It can be seen that the highest R_p^{max} value is achieved by the composition containing 3 wt.% of Sialon addition. An additional increment in filler concentration results in a reduction in the polymerization rate. Surprising results

were obtained in the case of the p^f . For fast polymerization reactions, as in the case of photochemical initiation, an increase in rate entails an increase in the degree of conversion as a result of a delay in volume relaxation relative to the chemical reaction. This also corresponds to an increase in the p^f value. However, p^f also depends on the mobility of the polymer chains (an increase in p^f indicates an increase in chain mobility). Figure 3d shows that Sialon addition affects the p^f value causing the final bond conversion, but this is independent of filler content. This may be related to the specific behavior of such a varnish composition. The viscosity of the dispersion is determined by the interaction between the filler and the varnish composition. The introduction of small amounts of Sialon reduces the mobility of growing macroradicals, which can be adsorbed on the filler surface. In both coatings, the final double bond conversion was high, in the range of 80%–95%.

3.3. Thermal and Mechanical Properties

The glass transition temperatures (T_g) of the polymer matrix depend on the free volume of the polymer, which is associated with the relationship between the filler and the polymer matrix [22]. A small amount of the fillers reduces the movement of the molecular segments in bisEA10, and therefore the T_g of the coatings increased; this can be due to the interactions between bisEA10 and the fillers (up to 5%), which appear to be strong enough to increase the glass transition temperature. The results obtained suggest that the reduction in the polymer chain mobility by AlN is stronger than that by Sialon. However, a higher content of fillers shows a weak interaction between the particles and the polymer; therefore, so as the free volume of the composites increased, T_g decreases. The positive effect of Sialon at its 5 wt.% loading is very slight and the deceleration effect mainly dominates. The results of mechanical measurements (hardness) of photopolymerized coatings are shown in Figure 4b. Noticeably, the hardness of the coatings of the photocured varnishes increases with increasing filler content by 15% (AlN) and 4% (Sialon), respectively, compared to the neat photocured coatings. This proves that fillers have an important role in enhanced UV-cured varnishes.

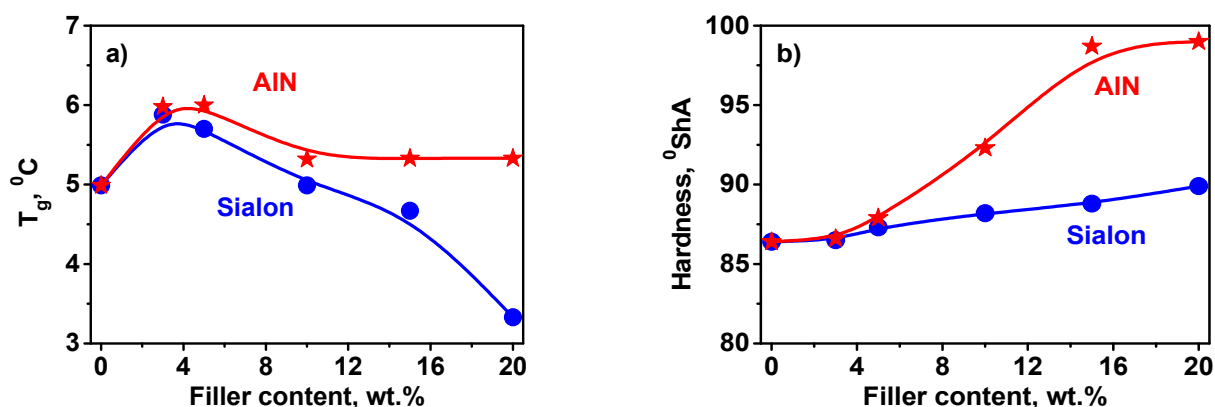


Figure 4. Glass transition T_g : (a) and hardness of coatings, (b) as a function of filler content.

The thermal stability can be estimated by TGA. Figure 5 demonstrates the weight loss and DTG thermograms of the varnish composite when heated to 600 °C. The weight loss of the system due to degradation is monitored as a function of temperature. The observed weight loss below 100 °C was due to evaporation water, volatile substances, or components of low molecular weight. The decomposition of the neat polymer appears in one main stage; the cleavage of the main chain is probably the major degradation path. A weight decrease between 100 and 500 °C is related to the decomposition of the organic group. The selected characteristic thermal parameters were the temperature of 10% ($T_{10\%}$), 50% ($T_{50\%}$) weight loss, and the maximum degradation rate temperature (T_{max}) (Table 1). From the TGA curve, it can be seen that the thermal stability of the coatings filled with Sialon and AlN was initially better than that of the pure matrix. For coatings without fillers, the onset temperature is 398 °C, while for coatings containing Sialon/AlN it increases to 400–403 °C.

It is worth mentioning that the presence of fillers leads to a slight enhancement of the decomposition stage, but the main degradation reaction is delayed. The residual mass of the pure matrix increases above the theoretical filler loading, suggesting that the fillers slightly impede diffusion of gaseous decomposition products.

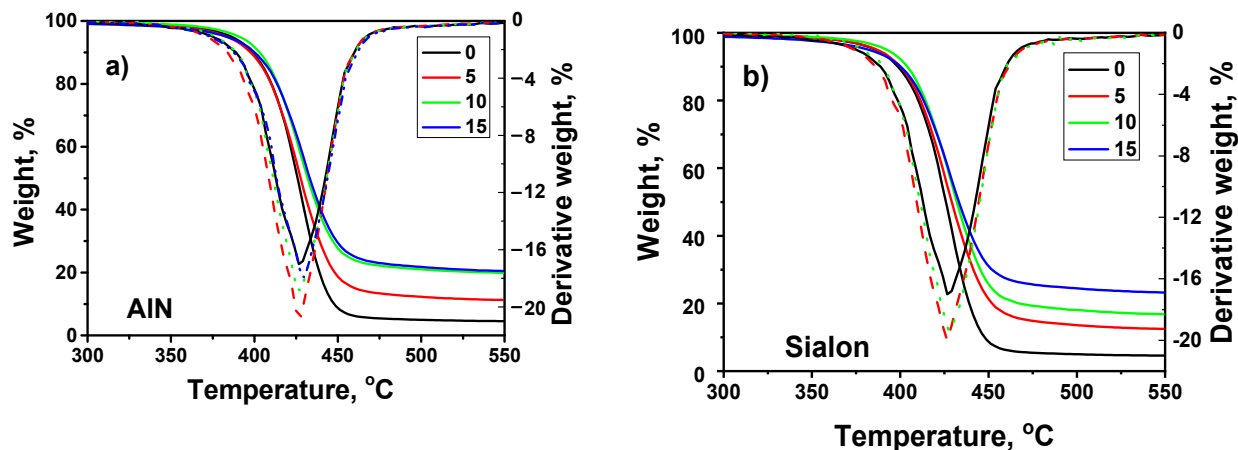


Figure 5. TGA and DTG curves for coatings containing: (a) Sialon, (b) AlN.

Table 1. Results of the thermal decomposition of Coatings.

Sample	Fillers Content [wt.%]	Residue [%]	Weight Loss Temperature [°C]		T_{max} [°C]
			$T_{10\%}$	$T_{50\%}$	
Sialon	0	4.51	398.7	425.8	423.0
	5	12.30	400.1	429.0	479.0
	10	16.63	404.1	432.0	427.7
	15	23.02	400.1	433.2	427.1
	20	24.89	403.1	433.9	426.9
AlN	5	11.14	397.7	427.7	426.7
	10	19.74	403.2	432.0	477.8
	15	20.26	400.0	433.2	479.0

3.4. FTIR-ATR Spectra

Figure 6 shows the FTIR-ATR spectra of the matrix and polymer coatings containing Sialon and AlN particles. The spectra of polymer are typical of polyacrylates with characteristic absorption peaks at 1718 cm^{-1} obtained from stretching vibration C=O and at 1100 cm^{-1} derived from the stretching bond C-O-C. The absorption band in the range of about $3200\text{--}3600\text{ cm}^{-1}$ corresponds to the vibrations of -OH groups present in one of the resins used. In filled coatings, the most visible and wide absorption band for AlN was noticed at 698 cm^{-1} , the spectrum showed a broad peak at 800 cm^{-1} in both cases results from Al-N stretching vibration. The extensive band at 3200 cm^{-1} corresponded to the N-H stretching vibrations of NH_2 groups, which is also related to the NH_2 band at 1543 cm^{-1} . We cannot observe residual absorption of the C=C bonds at 1636 cm^{-1} indicating complete conversion of the acrylate functions. This observation is consistent with the measurements of p^f (Figure 3d). AlN fillers are responsible for one strong and broad band, which peaked around 720 cm^{-1} , according to with data [23]. The peak at this wavelength widens and enlarges in polymer composites as the filler content increases. In coatings containing Sialon, there is an increase in absorption peaks in the range: $600\text{--}800\text{ cm}^{-1}$ with filler content. Absorption between 600 and 800 cm^{-1} is due to the Si-O, Al-N, and Al-O bonds in the sample. Absorption at 1040 cm^{-1} in Sialon filler, which indicates the presence of SiN_4 tetrahedra in the structure. The presence of filler in the compound is revealed by

the increase in the absorbance of bands in the range $1200\text{--}1500\text{ cm}^{-1}$ (peak overlapping) and in $600\text{--}825\text{ cm}^{-1}$ according to the increase in the filler content (Figure 6c). There are no displacements of the absorption peaks are observed, which confirms that the possible interactions of fillers with the polymer are fairly small.

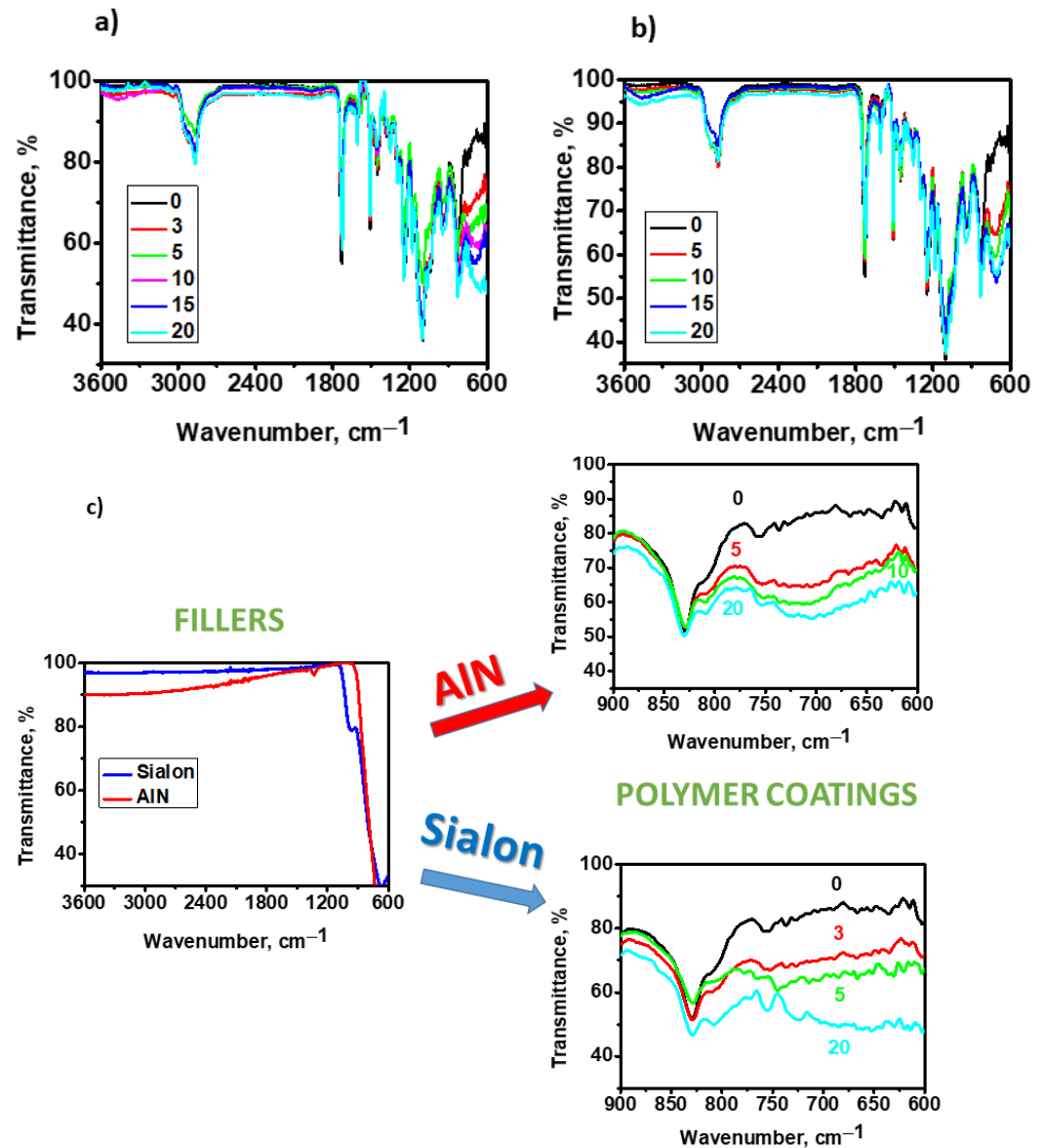


Figure 6. FTIR-ATR spectra of neat matrix and coatings containing (a) Sialon; (b) AlN and spectra of neat fillers and coatings (c). The numbers indicate filler content in wt.%.

3.5. Cross-Sectional Surface Morphology

The polymer matrix and the polymer composite containing the fillers had a smooth surface (Figure 1; surface on the first photograph) due to the fillers being covered by the polymer layer. Therefore, in order to investigate whether there is a good dispersion of fillers in the polymer matrix, SEM images of the cross-sectional surface of the samples (Figure 7) were taken.

SEM images show homogeneously distributed Sialon and AlN particles in the coatings for all filler contents; however, the materials of the coatings show large size nonspecific structures with rough surfaces and different shapes. Additionally, comparing the arrangement of Sialon and AlN fillers in the bulk, one can find a better dispersion and smaller particle size of AlN than Sialon in matrix. The AlN particles can be seen to be distributed

throughout the polymer matrix and this distribution was more uniform at higher filler content. The presence of the voids that appear in the photographs of the cross-sectional surface of the material is due to the fact that these specimens have been broken and there are still some holes left from the filler. This shows that the interactions between the filler and the polymer are not too strong and that the fillers are only “plugged” into the polymer matrix.

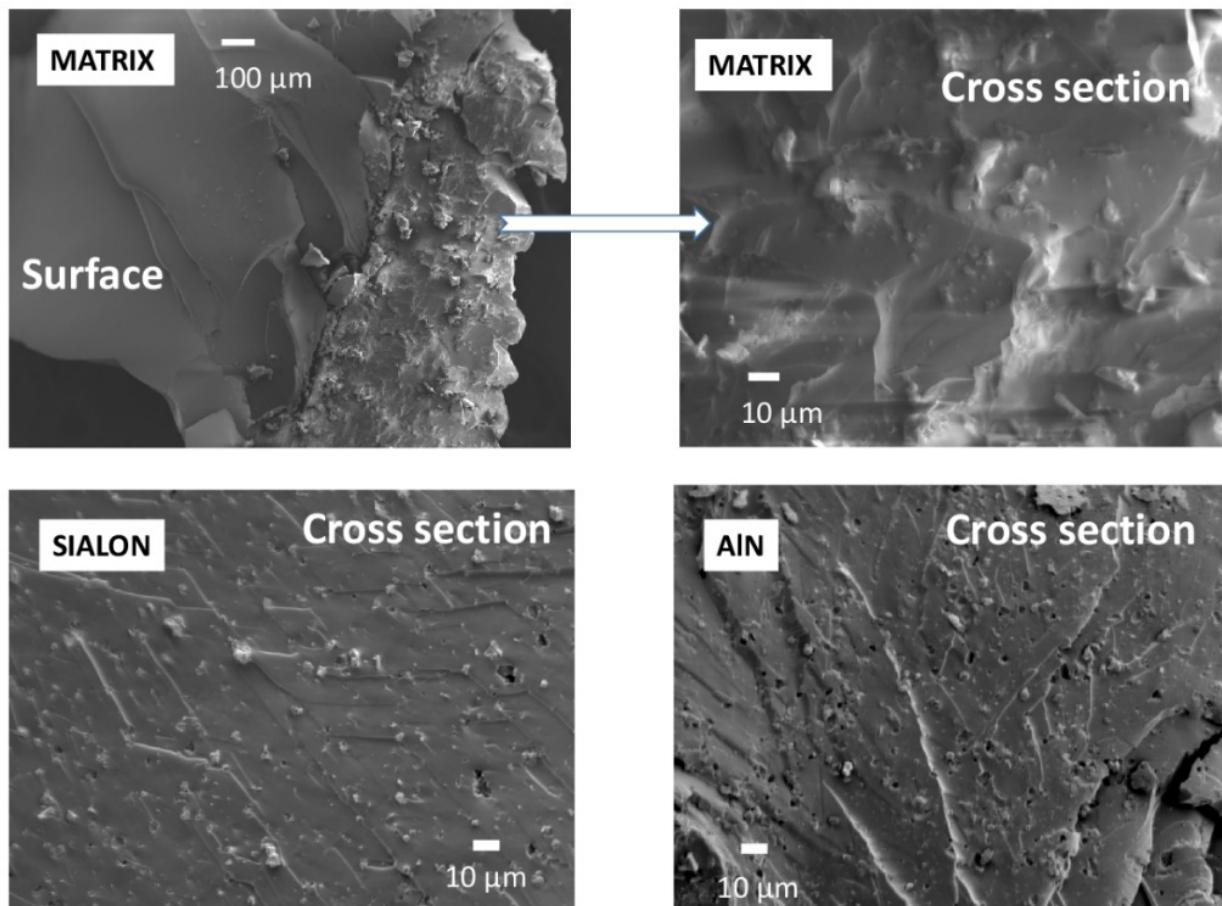
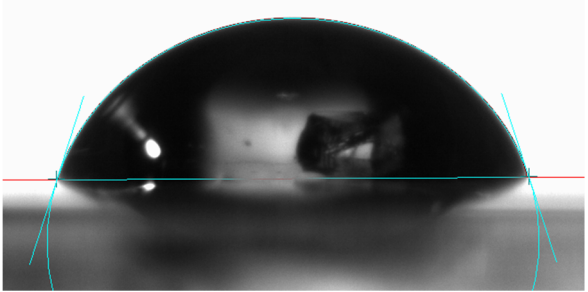
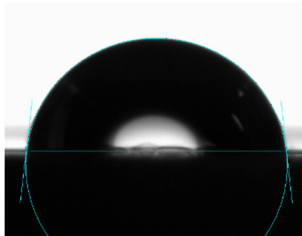
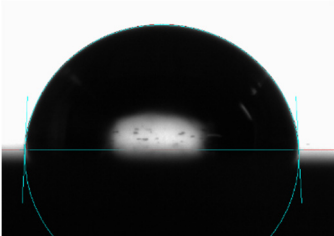
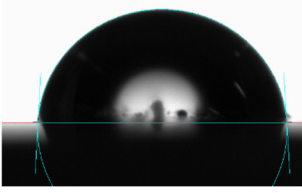
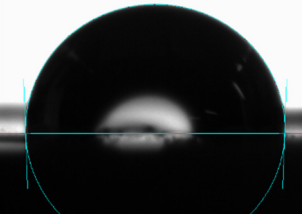
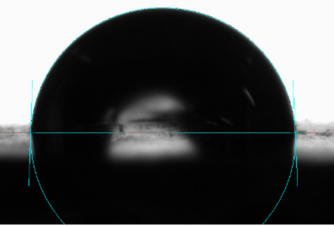
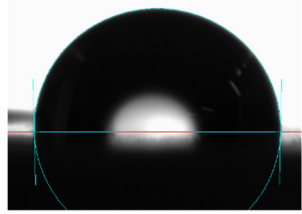
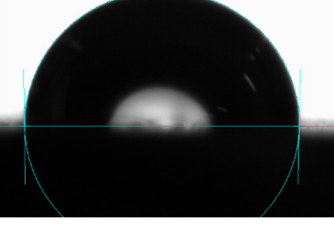


Figure 7. SEM micrographs of cross section of the sample composites containing AlN and Sialon particles. The filler content is 10 wt.%.

3.6. Contact Angle

The hydrophilic or hydrophobic character of the surface of the coating material can be evaluated by measuring the contact angle (θ_W). In our study, this parameter enabled the evaluation of changes in the hydrophobicity of the polymer matrix. The contact angle results are presented in Table 2. The contact angle determining surface wettability is the primary parameter that characterizes the shape of a droplet on a solid surface. The wettability can be explained as a characteristic controlled by intermolecular interactions that characterize the degree of wetting of the solid surface by a drop of liquid. When the surface of the solid is hydrophilic, θ_W will be lower than 90° , a hydrophobic material has θ_W greater than 90° ; θ_W values of the pure coatings are approximately 69° . The addition of both fillers changes the surface wettability. After the addition of 20% fillers, the wetting angle of the matrix increases above 90° , resulting in coatings with hydrophobic surface properties. This is highly desirable for varnish coatings as it reduces the adhesion of dust. As should be noted, coatings containing Sialon show a slightly better non-wetting property. In consequence, products coated with the varnishes can be used longer and it is easier to remove impurities from them [12].

Table 2. The image of contact angle θ_W .

Fillers Content [wt.%]	-	Contact Angle [$^\circ$] θ_W		
0	-	 $\theta_W = 69^\circ$		
-	$\theta_W [^\circ]$	Sialon	$\theta_W [^\circ]$	AlN
5	82		87	
10	87		78	
15	92		88	
20	97		91	

4. Conclusions

This work presents the results of an investigation of coatings based on poly ethoxylated bisphenol A diacrylate filled with Sialon and AlN. The polymer coatings were obtained by photopolymerization. The following main conclusions can be taken from the research:

- The addition of both types of fillers to the composition strongly influenced the photopolymerization rate and the viscosity of the photocurable composition.

- The addition of 20 wt.% Sialon and AlN increased the contact angle of the samples by approximately 40% and 31%, respectively, resulting in coatings with hydrophobic surface properties.
- The AlN filler embedded in the matrix reinforced the polymer (hardness) than Sialon, which was associated with better interaction between AlN and the polymer. The presence of fillers led to a slight enhancement of thermal stability of the coatings.

The research carried out will expand the knowledge on acrylate matrix polymer coatings containing Sialon and AlN. Modification of the properties of the studied materials may significantly contribute to a discovery of new applications for polymeric coatings with silicon-aluminum oxynitride and AlN obtained by the photopolymerization method.

Author Contributions: Conceptualization, M.R.; methodology, M.R.; software, M.R. and Ł.G.; validation, M.R. and Ł.G.; formal analysis, M.R. and P.M.; investigation, M.R., Ł.G. and K.S.; resources, M.R.; data curation, M.R.; writing—original draft preparation, M.R. and Ł.G.; writing—review and editing, M.R. and Ł.G.; visualization, M.R., P.M., A.M., A.L. and P.G.; supervision, Ł.G. and K.S.; project administration, M.R. and Ł.G.; funding acquisition, Ł.G. All authors have read and agreed to the published version of the manuscript.

Funding: This work was supported by the Ministry of Science and Higher Education. Authors would like to acknowledge the National Centre for Research and Development, Poland, grant number DWM/WPC2/285/2020, for help in SEM imaging.

Institutional Review Board Statement: Not applicable.

Informed Consent Statement: Not applicable.

Data Availability Statement: Not applicable.

Conflicts of Interest: The authors declare no conflict of interest.

References

1. Barick, P.; Saha, B.P. Effect of Boron Nitride Addition on Densification. Microstructure. Mechanical. Thermal. and Dielectric Properties of β -SiAlON Ceramic. *J. Mater. Eng. Perform* **2021**, *30*, 3603–3611. [[CrossRef](#)]
2. Ahmed, B.A.; Hakeem, A.S.; Laoui, T.; Khan, R.M.A.; Al Malki, M.M.; Ul-Hamid, A.; Khalid, F.A.; Bakhsh, N. Effect of precursor size on the structure and mechanical properties of calcium-stabilized sialon/cubic boron nitride nanocomposites. *J. Alloys Compd.* **2017**, *728*, 836–843. [[CrossRef](#)]
3. Falak, M.Z.; Ahmed, B.A.; Saeed, H.A.; Butt, S.U.; Hakeem, A.S.; Akbar, U.A. Spark Plasma Sintering of SiAlON Ceramics Synthesized via Various Cations Charge Stabilizers and Their Effect on Thermal and Mechanical Characteristics. *Crystals* **2021**, *11*, 1378. [[CrossRef](#)]
4. Hou, X.; Yue, C.; Guo, M.; Wang, X.; Zhang, M.; Chou, K.C. Synthesis, phase transformation and mechanical property of SiAlON ceramics from coal gangue. *J. Min. Met. A* **2014**, *50*, 47–55. [[CrossRef](#)]
5. Mohamedkhair, A.K.; Hakeem, A.S.; Drmosh, Q.A.; Mohammed, A.S.; Baig, M.M.A.; Ul-Hamid, A.; Gondal, M.A.; Yamani, Z.H. Fabrication and Characterization of Transparent and Scratch-Proof Yttrium/Sialon Thin Films. *Nanomater.* **2020**, *10*, 2283. [[CrossRef](#)]
6. Garrett, J.C.; Sigalas, I.; Wolfrum, A.K.; Herrmann, M. Effect of cubic boron nitride grain size in the reinforcing of α -Sialon ceramics sintered via SPS. *J. Eur. Ceram. Soc.* **2015**, *35*, 451–462. [[CrossRef](#)]
7. Hakeem, A.S.; Ali, S.; Jonson, B. Preparation and properties of mixed La-Pr silicate oxynitride glasses. *J. Non-Cryst. Solids* **2013**, *368*, 93–97. [[CrossRef](#)]
8. Ayas, E.; Kara, A. Novel electrically conductive α - β SiAlON/TiCN composites. *J. Eur. Ceram. Soc.* **2011**, *31*, 903–911. [[CrossRef](#)]
9. Kim, H.-H.; Lee, Y.-S.; Chung, D.; Kim, B.-J. Studies on Preparation and Characterization of Aluminum Nitride-Coated Carbon Fibers and Thermal Conductivity of Epoxy Matrix Composites. *Coatings* **2017**, *7*, 121. [[CrossRef](#)]
10. Wang, Q.; Cui, W.; Ge, Y.; Chen, K.; Xie, Z. Carbothermal synthesis of spherical AlN granules: Effects of synthesis parameters and Y_2O_3 additive. *Ceram. Int.* **2015**, *41*, 6715–6721. [[CrossRef](#)]
11. Gao, Z.; Wan, Y.; Xiong, G.; Guo, R.; Luo, H. Synthesis of aluminum nitride nanoparticles by a facile urea glass route and influence of urea/metal molar ratio. *Appl. Surf. Sci.* **2013**, *280*, 42–49. [[CrossRef](#)]
12. Robakowska, M.; Gierz, Ł.; Gojzewski, H. Sialon and Alumina Modified UV-Curable Coatings with Improved Mechanical Properties and Hydrophobicity. *Coatings* **2021**, *11*, 1424. [[CrossRef](#)]
13. Sadej, M.; Andrzejewska, E. Silica/aluminum oxide hybrid as a filler for photocurable composites. *Prog. Org. Coat.* **2016**, *94*, 1–8. [[CrossRef](#)]

14. Sadej, M.; Gojzewski, H.; Andrzejewska, E. Photocurable polymethacrylate-silica nanocomposites: Correlation between dispersion stability, curing kinetics, morphology and properties. *J. Polym. Res.* **2016**, *23*, 116. [[CrossRef](#)]
15. Sadej-Bajerlain, M.; Gojzewski, H.; Andrzejewska, E. Monomer/modified nanosilica systems: Photopolymerization kinetics and composite characterization. *Polymer* **2011**, *52*, 1495–1503. [[CrossRef](#)]
16. Sadej, M.; Gojzewski, H.; Gajewski, P.; Vancso, G.J.; Andrzejewska, E. Photocurable acrylate-based composites with enhanced thermal conductivity containing boron and silicon nitrides. *Express Polym. Lett.* **2018**, *12*, 790–807. [[CrossRef](#)]
17. Sadej, M.; Andrzejewska, E.; Kurc, B.; Gojzewski, H.; Jesionowski, T. Surface-dependent effect of functional silica fillers on photocuring kinetics of hydrogel materials. *J. Polym. Sci. Part A Polym. Chem.* **2014**, *52*, 3472–3487. [[CrossRef](#)]
18. Zhou, Y.; Yao, Y.; Chen, C.-Y.; Moon, K.; Wang, H.; Wong, C.-P. The use of polyimide-modified aluminum nitride fillers in AlN@PI/epoxy composites with enhanced thermal conductivity for electronic encapsulation. *Sci. Rep.* **2014**, *4*, 4779. [[CrossRef](#)]
19. Gojzewski, H.; Sadej, M.; Andrzejewska, E.; Kokowska, M. Nanoscale Young's modulus and surface morphology in photocurable polyacrylate/nanosilica composites. *Eur. Polym. J.* **2017**, *88*, 205–220. [[CrossRef](#)]
20. Chen, X.; Gonsalves, K.E. Synthesis and properties of an aluminum nitride/polyimide nanocomposite prepared by a nonaqueous suspension process. *J. Mater. Res.* **1997**, *12*, 1274–1286. [[CrossRef](#)]
21. Amorim, A.A.P.O.; Oliveira, M.G.; Mancini, M.C.; Sirqueira, A.S. Rheological, EMI and corrosion properties of epoxy coating with nanoparticle and conductive carbon black. *SN Appl. Sci.* **2021**, *3*, 236. [[CrossRef](#)]
22. Wu, S.-Y.; Huang, Y.-L.; Ma, C.-C.M.; Yuen, S.-M.; Teng, C.-C.; Yang, S.-Y. Mechanical, thermal and electrical properties of aluminum nitride/polyetherimide composites. *Compos. Part A Appl. Sci. Manuf.* **2011**, *42*, 1573–1583. [[CrossRef](#)]
23. Gilev, V.G. IR Spectra and Structure of Si–Al–O–N Phases Prepared by Carbothermal Reduction of Kaolin in Nitriding Atmosphere. *Inorg. Mater.* **2001**, *37*, 1041–1045. [[CrossRef](#)]